

## HYDRODYNAMIC CHARACTERISTICS OF BACKWARD FACING STEP FLOWS

\*Ching-Ruey LUO (Edward)

*Department of Civil Engineering, National Chi-Nan University, Nantou, Taiwan*

\*Author for Correspondence

### ABSTRACT

The flow over a backward facing step is often used as a test case for analyzing the performance of computational methods and turbulent models. It embodies several important aspects of turbulent flows, such as flow separation, recirculation, and reattachment, with such a higher Reynolds number. It is convenient if the separating point is set at the sharp corner of the step without the consideration of complexities arising from the movement of the sharp point. The analytically turbulent characteristic equations and their corresponding profiles of primary flow velocity, turbulent viscosity coefficient, turbulent shear stress, and turbulent kinetic energy are firstly derived and then compared with the available results from numerical models and/or experimental data. Some useful applications are also presented, discussed and concluded in this article.

**Keywords:** *Turbulence, Viscosity, Kinetic Energy, Flow Separation, Recirculation, Reattachment*

### Nomenclature

**E**=Specific energy

**Fr**=Froude number of inflow

**h**=Water depth of upstream (inflow)

**Hs**= Height of the given step

**k** =Turbulent kinetic energy

**u\*** =Turbulent shear velocity

**U** = Velocity of primary flow direction

$\bar{U}$  = The averaged velocity in the primary flow direction

**W** = Velocity of water depth direction

$\bar{W}$  = The averaged velocity in the primary flow direction

**x** = Primary flow direction

**z** = Water depth direction

### Greek Letters

$\epsilon$ =Turbulent energy dissipation rate

$\zeta$ =Variation of water depth

$\phi$  = Time scalar quantity which may stand for either temperature or species concentration

$\bar{\phi}$ =Time averaged scalar quantity for the flow characteristics

$\iota$ =Dissipation length scale

$\tau$ = Turbulent shear stress

$\nu$ = Turbulent viscosity coefficient

### INTRODUCTION

Separated flows associated with boundary discontinuity result in highly turbulent recirculating flows and are of considerable interest in many branches of engineering (Issa, 2005; Ting, 2005). Examples include, flow over surface discontinuities such as slots and steps, flow along the wall of rapidly expanding diffusers, and flow past blunt structures. Flow separation can cause significant energy losses. A backward facing step flow is often observed downstream of sand waves on river bed and the man-made hydraulic structures such as water gate and weirs. It is very important to investigate the structure of step flow in hydraulic engineering, because its velocity profiles vary rapidly and thus the mean-flow energy is highly dissipated there. It has been quite important to establish the turbulent velocities of such a water step flow.

## Review Article

The results of those turbulent velocities then will be used to obtain the other turbulent characteristic items such as turbulent viscosity coefficient, turbulent shear stress, turbulent kinetic energy, turbulent energy dissipation rate, and turbulent dispersion coefficient.

### 2. The Fundamental Equations of Two-dimensional Width Averaged Flow Model (2-DV)

#### 2.1. Width-averaged Quantities

Models for the vertical structure are obtained by width-averaging the original 3-D equations (Amano, 1987; DiZinno, 2013; Le and Moin, 1997; Poole, 2003; Speziale, 1988):

$$\bar{U} = \frac{1}{B(X,Z)} \int_{y_1}^{y_2} U dy \dots \dots \dots (1)$$

$$\bar{\phi} = \frac{1}{B(X,Z)} \int_{y_1}^{y_2} \phi dy \dots \dots \dots (2)$$

When the hydrostatic pressure approximation is not used, these equations read:

#### 2.1.1 Mass Conservation: Continuity Equation

$$\frac{\partial}{\partial x} (B\bar{U}) + \frac{\partial}{\partial z} (B\bar{W}) = 0 \dots \dots \dots (3)$$

#### 2.1.2 Momentum Conservation: Navier-Stoke Equations

##### (a) x-momentum

$$\frac{\partial (B\bar{U}^2)}{\partial x} + \frac{\partial (B\bar{U}\bar{W})}{\partial z} = -gB \frac{\partial \xi}{\partial x} - \frac{B}{\rho_0} \frac{\partial p_d}{\partial x} + \frac{\tau_{wx}}{\rho_0} + \frac{1}{\rho_0} \frac{\partial (B\bar{\tau}_{xx})}{\partial x} + \frac{1}{\rho_0} \frac{\partial (B\bar{\tau}_{xy})}{\partial z} + \frac{1}{\rho_0} \frac{\partial}{\partial x} \int_{y_1}^{1/2} \rho (W - \bar{W})(U - U dy) \dots \dots \dots (4)$$

##### (b) z-momentum

$$\frac{\partial (B\bar{W}^2)}{\partial z} + \frac{\partial (B\bar{U}\bar{W})}{\partial x} = \frac{B}{\rho_0} \frac{\partial p_d}{\partial z} + \frac{\bar{p} - p_0}{\rho_0} \xi B + \frac{\tau_{wz}}{\rho_0} + \frac{1}{\rho_0} \frac{\partial (B\bar{\tau}_{xz})}{\partial x} + \frac{1}{\rho_0} \frac{\partial (B\bar{\tau}_{zz})}{\partial z} + \frac{1}{\rho_0} \frac{\partial}{\partial x} \int_{y_1}^{y_2} \rho (U - \bar{U})(W - \bar{W}) dy + 1\rho_0\partial\partial zy1y2\rho W-W2dy \dots \dots \dots (5)$$

#### 2.1.3 Scalar Transport Equation

$$\frac{\partial (B\bar{U}\bar{\phi})}{\partial x} + \frac{\partial (B\bar{W}\bar{\phi})}{\partial z} = \frac{Bq_s}{\rho_0} + \frac{1}{\rho_0} \frac{\partial (B\bar{I}_x)}{\partial x} - \frac{1}{\rho_0} \frac{\partial (B\bar{I}_z)}{\partial z} + \frac{1}{\rho_0} \frac{\partial}{\partial x} \int_{y_1}^{y_2} \rho (U - \bar{U})(\phi - \bar{\phi}) dy + \frac{1}{\rho_0} \frac{\partial}{\partial x} \int_{y_1}^{y_2} \rho (U - \bar{U})(\phi - \bar{\phi}) dy + 1\rho_0\partial\partial zy1y2\rho W-W\phi-\phi dy \dots \dots \dots (6)$$

#### 2.1.4 k-ε Equations

##### (a) k-equation

$$\bar{U} \frac{\partial k}{\partial x} + \bar{W} \frac{\partial k}{\partial z} = \frac{\partial}{\partial x} \left( \frac{v_t}{\sigma_k} \frac{\partial k}{\partial x} \right) + \frac{\partial}{\partial z} \left( \frac{v_t}{\sigma_k} \frac{\partial k}{\partial z} \right) + P_k - \epsilon \dots \dots \dots (7)$$

##### (b) ε-equation

$$\bar{U} \frac{\partial \epsilon}{\partial x} + \bar{W} \frac{\partial \epsilon}{\partial z} = \frac{\partial}{\partial x} \left( \frac{v_t}{\sigma_\epsilon} \frac{\partial \epsilon}{\partial x} \right) + \frac{\partial}{\partial z} \left( \frac{v_t}{\sigma_\epsilon} \frac{\partial \epsilon}{\partial z} \right) + \frac{\epsilon}{k} (C_{1\epsilon} - C_{2\epsilon}) \dots \dots \dots (8)$$

and

$$P_k = v_t \left[ 2 \left( \frac{\partial \bar{U}}{\partial x} \right)^2 + 2 \left( \frac{\partial \bar{W}}{\partial z} \right)^2 + \left( \frac{\partial \bar{U}}{\partial z} + \frac{\partial \bar{W}}{\partial x} \right)^2 \right] \dots \dots \dots (9)$$

$$c_{1\epsilon} = 1.44; c_{2\epsilon} = 1.92; c_\mu = 0.09; \sigma_k = 1.0; \sigma_\epsilon = 1.3;$$

#### 2.1.5 Dissipation Length Scale

$$l^2 = \frac{d}{dz} \left( \frac{1}{k} \frac{dk}{dz} \right) + \frac{7}{2} \left( \frac{1}{k} \frac{dk}{dz} \right) + k - F_1 - F_2 = 0 \dots \dots \dots (10)$$

$$F_1 = \left( \frac{\sigma_k c_\mu^{1/2}}{k^2} \right) \left( \frac{3}{2} - C_{1\epsilon} \right) \left( 1 - \frac{P_{kv}}{\epsilon} \right) \dots \dots \dots (11)$$

$$F_2 = \frac{3}{4} \left( \frac{1}{k} \right)^2 \left( \frac{dk}{dz} \right)^2 \dots \dots \dots (12)$$

$$P_{kv} = -\bar{u}'w' \frac{\partial \bar{U}}{\partial z} + v_{tz} \left( \frac{\partial \bar{U}}{\partial z} \right)^2 = 2v_{tz} \left( \frac{\partial \bar{U}}{\partial z} \right)^2 \dots \dots \dots (13)$$

$$\text{If } \left| \frac{h}{k} \frac{dk}{dz} \right| \leq 1, P_{kv} = 2v_{tz} \left( \frac{\partial \bar{U}}{\partial z} \right)^2 \dots \dots \dots (14)$$

## Review Article

$$\frac{d\bar{U}}{dz} = -\sqrt{1 - F_1} \text{ with } P_{kv} = 0 \dots\dots\dots(15)$$

$$\bar{U} \frac{d^2 \bar{U}}{dz^2} = 1 - F_1 - F_2 \dots\dots\dots(16)$$

$$\int \bar{U} \frac{d^2 \bar{U}}{dz^2} dz = 0 \dots\dots\dots(17)$$

### 2.2 Kinematic Boundary Conditions

#### 2.2.1 Non-slip boundary

$$\bar{U} \frac{\partial \xi}{\partial x} - \bar{W} = 0 \dots\dots\dots(18)$$

#### 2.2.2 Wall shear stress:

$$\tau_w = \frac{\rho g}{C_z^2} (\bar{U}^2 + \bar{W}^2) \dots\dots\dots(19)$$

#### In x-direction

$$\tau_{wx} = \frac{\bar{U}}{\sqrt{\bar{U}^2 + \bar{W}^2}} \tau_w \dots\dots\dots(20)$$

#### In z-direction

$$\tau_{wz} = \frac{\bar{W}}{\sqrt{\bar{U}^2 + \bar{W}^2}} \tau_w \dots\dots\dots(21)$$

#### 2.2.3 Variation of water depth

$$\text{Pressure in depth: } \frac{\partial P_d}{\partial z} = (\bar{\rho} - \rho_0)g \dots\dots\dots(22)$$

#### 2.2.4 Variation of water surface

$$\text{Pressure in flow profile: } \frac{\partial P_d}{\partial x} = g \frac{\partial}{\partial x} \int_{-h}^{\xi} (\bar{\rho} - \rho_0) dz \dots\dots\dots(23)$$

### 3. Analytical Solutions of Turbulent Characteristics

Separated flows associated with boundary discontinuously result in highly turbulent recirculating flows. Flow separation can cause significant energy loss. The optimum performance of fluid machinery can be predicted by a better understanding of the characteristics of flow separation. Numerous studies researched on understanding parameters which affect the reattachment process over a backward-facing step have been done. The effect of Reynolds number, the inlet condition ratio of boundary layer thickness to step heights and the effect of streamline curvature on the reattachment length were examined in the experiment (Adams, 1984; Durst, 1981; Honami, 1986). The idea of plane shear layer jets is used to solve the analytical primary velocity profiles with continuity equation and equations of motion in primary flow direction with the definition of backward-facing step sketched in Figure 1. The wall frictions are neglected. The turbulent viscosity coefficient, turbulent kinetic energy, energy dissipation rate, and turbulent dispersion coefficient are solved by 2-D momentum equations and the k-ε width-averaged relationship.

#### 3.1 Characteristics of Stream within the Separation Flow

Regressions of the data (Adams, 1984; Durst, 1981; Honami, 1986; Rajasekaran, 2011; Surana, 2007; Gao, 1992; Nakagawa, 1987), the following results are obtained:

##### 3.1.1 Kinetic energy dissipation

$$\frac{\Delta E}{E} = (a_1 F_r + a_2)(S)^{a_3} \left\{ 1 - \text{Exp} \left[ -a_4 \left( \frac{x}{H_s} \right) \right] \right\} \dots\dots\dots(24)$$

where  $S = h/H_s$ ,  $a_1 = 0.70$ ,  $a_2 = 0.80$ ,  $a_3 = 0.96$ ,  $a_4 = 0.11$ , and  $F_r$ : Froude number of the inlet and less or equal 1.0.

##### 3.1.2 Reattachment length

$$\frac{x_R}{H_s} = a \cdot \text{Exp}[-b \cdot Re] \dots\dots\dots(25)$$

where  $x_R$  = the reattachment length,  $a = 36.68$ ,  $b = 0.194$ ,  $Re$ : the Reynolds number of inlet.

## Review Article

### 3.1.3 Profile of the streamline within the separation flow

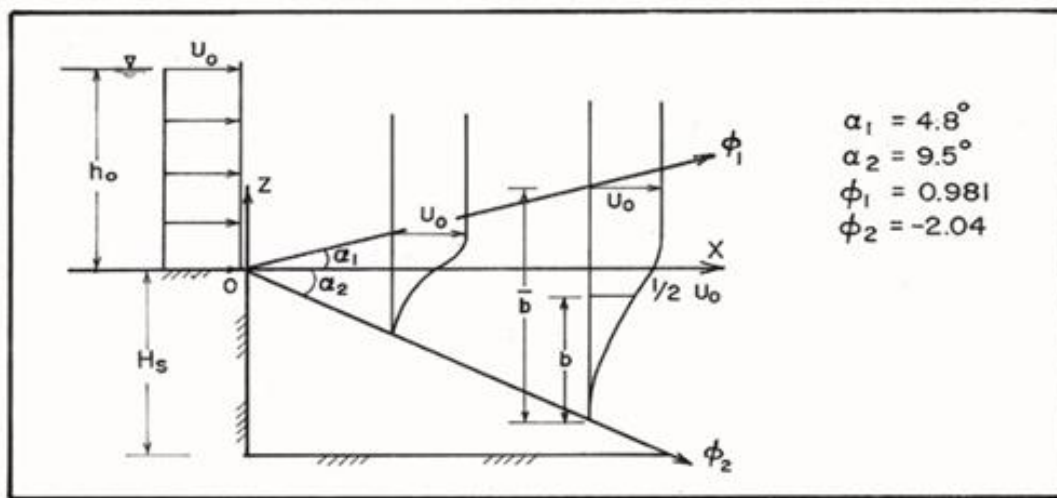


Figure 1: Definition Sketch of Plane Turbulent Shear Layers

For plotting the streamline of  $\psi=0$ , the profile with separation zone is:

$$\left(\frac{H_0}{H_s}\right) = A \left(\frac{x_r}{H_s}\right)^2 + B \left(\frac{x_r}{H_s}\right) + C \quad \dots\dots\dots(26)$$

where  $H_0$  is the height of the position for  $\psi=0$ , at the downstream and it is calculated from the bed and  $x_r$  is less or equal to  $x_R$ ;  $A=-0.04$ ,  $B=0.08$ , and  $C=1.0$ .

### 3.2 Analytical Solutions of Turbulent Characteristics

#### 3.2.1 Primary velocity profile

Let us consider a plane jet of large or semi-infinite height leaving a thin plate and flow over a stagnant mass of the same fluid as defining in Figure 1, the upper limit angle with  $\alpha_1=4.80^\circ$  for  $U/U_0=1.0$ , and  $\alpha_2=9.50^\circ$  for  $U/U_0=0.0$ .

The intense shear at the surface of velocity discontinuity induces turbulence and the stagnant fluid is accelerated whereas a portion of the jet losses some momentum.

The thickness of the fluid layer affected by this exchange of momentum is known as the mixing layer or free shear layer and its thickness at any  $x$ -station could be denoted by  $\bar{b}$  and it grows continuously with  $x$ . We also can define  $b$  where  $U/U_0=0.5$ .

$$\bar{b} = 0.263x \quad \dots\dots\dots(27)$$

$$b = 0.115x \quad \dots\dots\dots(28)$$

and

$$\frac{U}{U_0} = \text{Exp} \left[ -0.01 \left( \frac{z-H_0}{b} \right)^2 \right] - 1, \text{ if } z \leq H_0 \quad \dots\dots\dots(29)$$

$$\frac{U}{U_0} = 1 - \text{Exp} \left[ -0.787 \left( \frac{z-H_0}{b} \right)^2 \right], \text{ if } z \geq H_0 \quad \dots\dots\dots(30)$$

$$\bar{U} = U \left[ 1 - \left( \frac{\sqrt{\pi}}{2} \right) \left( \frac{b}{h} \right) \text{erf} \left( 0.887 \left( \frac{z-H_0}{b} \right) \right) \right] \quad \dots\dots\dots(31)$$

$$U_0 h_0 = \bar{U} h \quad \dots\dots\dots(32)$$

where  $U = 0$  happens at the streamline  $\psi=0$  or at the height of  $H=H_0$  and we also can see that  $\alpha_2=9.50^\circ$  means the horizontal position of  $\psi=0$  from the starting point of backward-facing step will be six times of this step height and this phenomena shows the quite good property as in Eq. (26).

#### 3.2.2 Turbulent viscosity coefficient

$$\nu_{tz} = u_*^2 \left( 1 - \frac{z}{h} \right) \frac{b^2}{1.54 U_1 (z-H_0) \text{Exp} \left[ -0.787 \left( \frac{z-H_0}{b} \right)^2 \right]} \quad \dots\dots\dots(33)$$

## Review Article

### 3.2.3 Turbulent shear stress

$$\tau_{xz} = \nu_{tz} \partial U / \partial z = u_*^2 \left(1 - \frac{z}{h}\right) \dots \dots \dots (34)$$

### 3.2.4 Turbulent kinetic energy

(1) if  $z \geq H_0$

$$\bar{k} = \frac{1}{2} \left\{ 0.027 \left( \frac{\nu}{U_1 h_1} \right)^{1/4} U_1^2 \left[ \frac{120(H_s - Z)}{x} - 10 \ln x - \ln \left( \frac{10H_s}{19Z} \right) + \left( \frac{54}{10h} + \frac{5}{H_s} + \frac{10Z}{hH_s} \right) x - \frac{Z}{hX} \left( 2.39H_s - 179Z - 60H_s 2Z + x 25H_s h - x 330h H_s 2 - 0.06U_1 h 1 \nu 14U_1 21 - \pi 2b \operatorname{erf} 0.887h - H_0 b 2, \dots \dots \dots (35) \right. \right.$$

(2) if  $Z \leq H_0$

$$\bar{k} = \frac{1}{2} \left\{ 0.027 \left( \frac{\nu}{U_1 h_1} \right)^{1/4} U_1^2 \left[ \frac{120(H_s - Z)}{x} - 10 \ln x - \ln \left( \frac{10H_s}{19Z} \right) + \left( \frac{54}{10h} + \frac{5}{H_s} + \frac{10Z}{hH_s} \right) x - \frac{Z}{hX} \left( 2.39H_s - 179Z - 60H_s 2Z + x 25H_s h - x 230h H_s 2 - 32.5U_1 h 1 \nu 14U_1 2 \operatorname{Exp} - 0.01Z - H_0 b - 12, \dots \dots \dots (36) \right. \right.$$

### 3.2.5 Turbulent dispersion coefficient

$$\bar{D}_T = 1.10 \left( \frac{U_0^2}{u_*} \right) \left\{ (0.013) \frac{b^7}{(h-H_0)^6} - (0.041) \frac{b^6}{(h-H_0)^5} - \frac{b^5}{(h-H_0)^4} \left[ 0.018 + 0.017 \operatorname{erf}(0.887) \left( \frac{h-H_0}{b} \right) \right] + b 4h - H_0 30.132 - 0.03 \operatorname{erf} 0.887h - H_0 b + b 2h - H_0 0.3 \operatorname{erf} 0.887h - H_0 b - b 3h - H_0 2 \cdot 0.045 \operatorname{erf} 0.887h - H_0 b + 0.149 \dots \dots \dots (37) \right.$$

### 3.2.6 Turbulent kinetic energy dissipation

$$\frac{\Delta E_k}{E_{k0}} = \frac{U_0^2 - \bar{U}^2}{U_0^2} \dots \dots \dots (38)$$

## 4. Comparison and Discussion

### 4.1 Comparisons

#### 4.1.1 Primary Velocity

The comparisons of the primary velocity between analytical and numerical results (J. Gao 1993, and H.W. Liepmann 1947) of Froude number less or equal to 1.0 are showed in Figs. 2 and 3. The high qualities of the agreements are obtained.

#### 4.1.2 Turbulent Shear Stress

The comparisons of turbulent shear stress between analytical and experimental results (J. Gao 1993) is plotted in Figure 4. Obvious agreement is expressed and valid.

#### 4.1.3 Turbulent Kinetic Energy

The comparisons of turbulent kinetic energy between analytical and experimental results (J. Gao 1993) is plotted in Figure 5. Relevant agreement is presented and valid.

### 4.2 Discussion

When the flow situations in the entrance of upstream of the backward-facing steps are orifice, which controls the inflow by critical depth, and there are no tail water effects of free jump to the normal depth, the results will be different to the ones (Gao, 1993).

There are three cases of this orifice in upstream with no tail water in downstream:

#### (1) Isolated Nappe Flow

It exhibits alternating sub- and supercritical flow or be entirely. If the inflow is in sub-critical case, a hydraulic jump appears just beyond the point of impact of the nappe. The water depth reaches its minimum value  $z_{1j}$  jump appears just beyond the point of impact of the nappe. The water depth reaches its

## Review Article

minimum value  $z_1$  at the point of impact of the nappe and a water cushion of depth,  $z_p$  forms at the inner edge of the step.

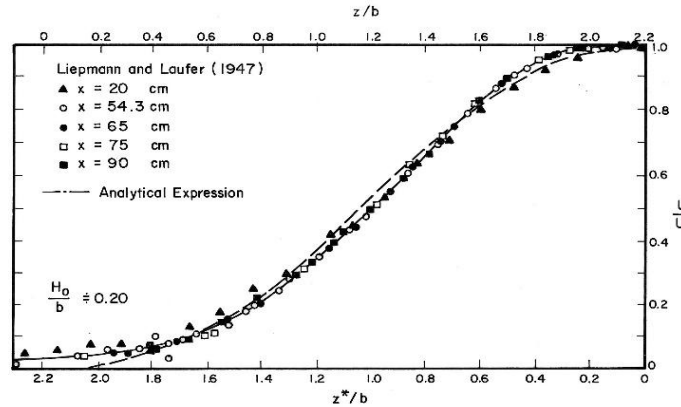


**Figure 2: Comparisons of Dimensionless Velocity Profile between Analytical and Experimental Results**

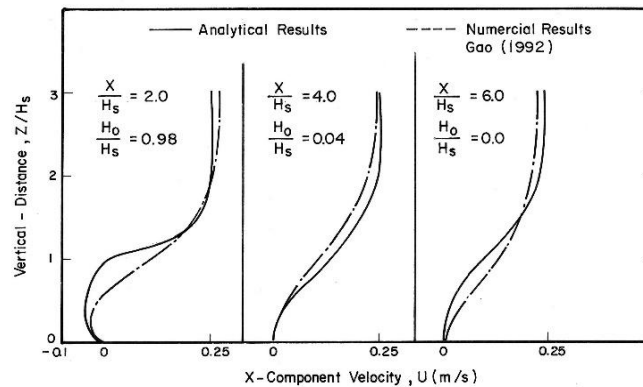


**Figure 3: Comparisons of X-Component Velocity between Analytical and Numerical Results for  $U_1=0.24$  m/s;  $S=0.34$ ;  $Fr_1=0.32$  and  $Re=14,000$**

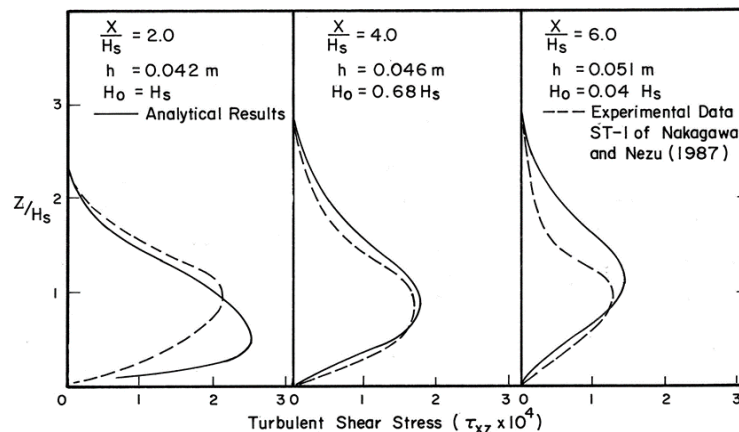


**Figure 4: Comparisons of Turbulent Shear Stress between Analytical and Experimental Results for Backward-facing Steps with  $U_1=0.243$  m/s,  $h_1=0.038$  m,  $H_s=0.02$  m**



## Review Article

After certain distance,  $z_2$ , the conjugate depth of  $z_1$ , becomes subcritical; finally, the normal depth,  $z_n$ , reduces (Ohtsu, 1991). The following equations (Rand, 1955) are given,

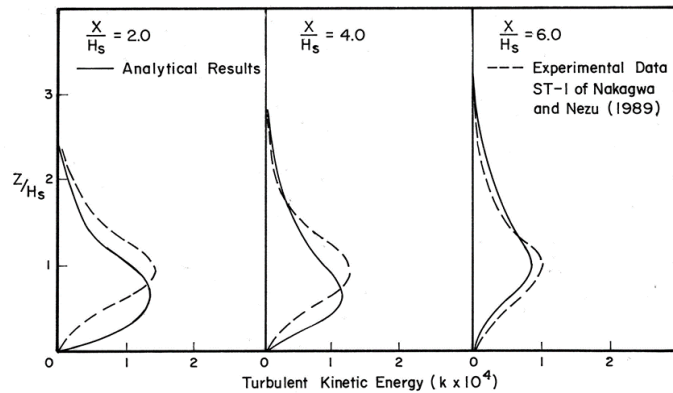


**Figure 5: Comparisons of Turbulent Kinetic Energy between Analytical and Experimental Results for Backward-facing Steps with  $U_1=0.243$  m/s,  $h_1=0.038$  m,  $H_s=0.02$  m**

$$\frac{z_1}{H_s} = 0.54 \left( \frac{q^2}{gH_s^3} \right)^{0.425} \dots\dots\dots(39)$$

$$\frac{z_2}{H_s} = 1.66 \left( \frac{q^2}{gH_s^3} \right)^{0.270} \dots\dots\dots(40)$$

$$\frac{z_p}{H_s} = \left( \frac{q^2}{gH_s^3} \right)^{0.220} \dots\dots\dots(41)$$

### (2) Partial Nappe Flow

In this case, the flow makes the nappe not fully impinge on the step surface. The depth,  $z_p$ , can still be seen and the partial nappe flow will disperse with considerable turbulence. Flow is supercritical down the whole length of the step. In nappe flow, energy is dissipated in two stages. The first stage is on impact with the flat surface. Then, the next stage is in the turbulence created by dispersal of the nappe with or without the formation of a hydraulic jump. By regressing the data (Peyras, 1992), we have:

$$(1 - T_1)^{-1} = 0.245 F_{r*}^{-0.521} i^{-0.476} \dots\dots\dots(42)$$

$$T_2 = 0.311 F_{r*}^{0.261} i^{-0.476} \dots\dots\dots(43)$$

$$T_1 = \frac{E_0 - E_1}{H_s}; T_2 = \frac{z_1}{H_s} \dots\dots\dots(44)$$

and  $i$  is the slope of unit still length or slope of spillway.

### (3) Skimming Flow

It occurs at moderate to high discharge. No nappe is visible and the step is submerged beneath a strong, relatively smooth current. The skimming flow gives a much less efficient energy dissipator with the detailed theory of skimming flow based on experiments (Rajaratnam, 1990).

Some studies (Wang, 2014; Chen, 2012) also research the situations as mentioned above. Physically and theoretically speaking, the turbulent effects including turbulent viscosity within boundary layer is very significant for forming the turbulent kinetic energy and energy dissipation rate which results in the turbulent shear stresses in order to entrain and uplift the bed material in suspension and to deform the original bed form into ripples or dunes even anti-dunes (Luo, 1993).

## CONCLUSION

The comparisons of velocity profiles, turbulent shear stress and turbulent kinetic energy among analytical, experimental and numerical results with standard parameter values present obviously good agreement with Froude number less or equal to unity. The useful regression equations for application are showed in this study.

## Review Article

### REFERENCES

- Adams EC et al., (1984).** Experiments on the structure of turbulent reattaching flow. Stanford University Report MD-39.
- Amano RS and Goal P (1987).** Investigation of third-order closure model of turbulence for the computation of incompressible flows in a channel with a backward-facing step. *Transactions of the ASME* **109** 424-428.
- Chen YL and Lee KT (2012).** Flow pattern simulation and resistance analysis in step channels. *Journal of Chinese Soil and Water Conservation* **43**(2) 97-108.
- DiZinno N and Vradis G (2013).** A strongly implicit method for the solution of transient incompressible viscous flow problems, *51st AIAA Aerospace Sciences Meeting including the New Horizons Forum and Aerospace Exposition* Grapevine (Dallas/Ft. Worth Region), Texas.
- Durst F and Tropea C (1981).** Turbulent, backward-facing step flows in two-dimensional ducts and channels. *Proceedings of 3<sup>rd</sup> Symposium of Turbulent Shear Flows* **18** 1-6.
- Davis J Gao (1992).** *Calculation of Energy Dissipation due to an Abrupt Bed Drop in Openchannel*. Master Thesis No. WA-92-8, Asian Institute of Technology, Bangkok, Thailand.
- Honami S and Nakajo I (1986).** A reattaching shear layer to the curved surfaces over a backward-facing step, ASME paper 86-WA/FE-9.
- Issa R, Lee ES and Violeau D (2005).** Incompressible separated flows simulations with the smoothed particle hydrodynamics gridless method. *International Journal for Numerical Methods in Fluids* **47** 1101-1106.
- Le H, Moin P and Kim J (1997).** Direct numerical simulation of turbulent flow over a backward-facing step. *Journal of Fluid Mechanics* **330** 349-374.
- Liepmann HW and Laufer J (1947).** Investigation of free turbulent mixing, N.A.C.A., Tech. Note 1257.
- Luo CR (1993).** Hydrodynamic characteristics in non-uniform channels, Dissertation No. WA 93-1, Asian Institute of Technology, Thailand.
- Nakagawa H and Nezu I (1987).** Experimental investigation on turbulent structure of backward-facing step flow in an open channel. *Journal of Hydraulic Research, IAHR* **106**(1) 67-88.
- Ohtsu and Yasuda Y (1991).** Transition from supercritical to subcritical flow at an abrupt drop. *Journal of Hydraulic Research* **29**(3).
- Peyras L, Royet P and Degouttel G (1992).** Flow and energy dissipation over stepped Gabion Weirs. *Journal of Hydraulic Engineering ASCE* **118**(5).
- Poole RJ and Escudier MP (2003).** Turbulent flow of non-Newtonian liquids over a backward-facing step. *Journal of Non-Newtonian Fluid Mechanics* (Elsevier) **109** 193-230.
- Rajasekaran J (2011).** On the flow characteristics behind a backward-facing step and the design of a new axisymmetric model for their study, Thesis of Master of Applied Science Graduate Department of Aerospace Engineering, University of Toronto.
- Rajaratnam N (1990).** Skimming flow in stepped spillways. *Journal of Hydraulic Engineering ASCE* **116**(4).
- Rand W (1955).** Flow geometry at straight drop spillways *Proceeding ASCE* 81.
- Speziale CG and Ngo T (1988).** Numerical solution of turbulent flow past a backward-facing step using a nonlinear k- $\epsilon$  model. *International Journal of Engineering Science* **10** 1099-1112.
- Surana A, Jacobs GB and Haller G (2007).** Extraction of separation and attachment surfaces from Three-Dimensional Steady Shear Flows. *AIAA Journal* **45**(6).
- Ting TS, Prakash M, Cleary PW and Thompson MC (2005).** Simulation of high Reynolds number flow over a backward facing step using SPH. *ANZIAM Journal* **47**(EMAC) C292-C309.
- Wang S, Burton D, Sheridan J and Thompson MC (2014).** Characteristics of Flow over a Double Backward-Facing Step, *19th Australasian Fluid Mechanics Conference Melbourne, Australia*.